The 2nd Spitzer Conference: Infrared Diagnostics of Galaxy Evolution
ASP Conference Series, Vol. 381, ©2008
Ranga-Ram Chary, Harry I. Teplitz, Kartik Sheth, eds.

Spitzer Observations of High Redshift Radio Galaxies

N. Seymour,[1] D. Stern,[2,1] C. De Breuck,[3] J. Vernet,[3] R. Fosbury,[3] A. Rettura,[4,3] A. Zirm,[5] B. Rocca-Volmerange,[4] M. Lacy,[1] H. Teplitz,[1] A. Dey,[6] M. Dickinson,[6] W. van Breugel,[7] G. Miley,[8] H. Röttgering,[8] P. Eisenhardt,[2] P. McCarthy,[9], F. De Breuck[3] and L. Vernet[3]

[1] *Spitzer Science Center, California Institute of Technology, Mail Code 220-6, 1200 East California Boulevard, Pasadena, CA 91125*
[2] *Jet Propulsion Laboratory, California Institute of Technology, Pasadena, CA 91109*
[3] *European Southern Observatory, Karl Schwarzschild Strasse, D-85748 Garching, Germany*
[4] *Institute d'Astrophysique de Paris, 98bis Bd Arago, 75014 Paris, France*
[5] *Space Telescope Science Institute, 3700 San Martin Drive, Baltimore, MD 21218*
[6] *National Optical Astronomy Observatory, Tucson, AZ 85719*
[7] *Institute of Geophysics and Planetary Physics, Lawrence Livermore National Laboratory, Livermore, CA 94551*
[8] *Leiden Observatory, University of Leiden, P.O. Box 9513, 2300 RA Leiden, Netherlands*
[9] *Carnegie Observatories, 813 Santa Barbara Street, Pasadena, CA 91101*

Abstract. We present the results of a comprehensive *Spitzer* survey of 70 radio galaxies across $1 < z < 5.2$. Using IRAC, IRS and MIPS imaging we determine the rest-frame AGN contribution to the stellar emission peak at 1.6μm. The stellar luminosities are found to be consistent with that of a giant elliptical with a stellar mass of $10^{11-12}\,M_{\odot}$. The mean stellar mass remains constant at $10^{11.5}\,M_{\odot}$ up to $z = 3$ indicating that the upper end of the mass function is already in place at redshift 3. The mid-IR luminosities imply bolometric IR luminosities that would classify most sources as ULIRGs. The mid-IR to radio luminosity generally correlate implying a common origin for these emissions. The ratio is higher than that found for lower redshift, *i.e.* $z < 1$, radio galaxies.

1. Introduction

Classical radio galaxies are the quintessential type II active galactic nuclei (AGN): accreting super-massive black holes that have their continuum emission in the UV/optical/NIR absorbed by dust, thus primarily giving them the appearance of *normal* star-forming galaxies at these wavelengths. The main evidence that they host super-massive black holes comes from the high luminosities of their radio 'lobes' that are fed by radio jets originating from the host galactic nuclei (Rees 1978). The lobe spatial extents (tens of mega-parsecs) and the lumi-

nosities ($L_{1.4\mathrm{GHz}} \geq 10^{25}\,\mathrm{WHz}^{-1}$) rule out emission from star-formation. To be more precise radio galaxies are Faranoff-Riley type II objects with edge-brightened radio lobes. In terms of the orientation unification scheme for AGN (Antonucci 1984) radio galaxies are analogous to radio loud quasars obscured in the UV/optical/NIR.

Due to their large radio luminosities, radio galaxies were the predominant way to probe the distant universe until the advent of ultra-deep optical surveys in the last decade. In fact, radio galaxies were the first galaxies to be found above redshifts 1, 2, 3 and 4 (e.g., Lacy et al. 1994). Since their first discovery it has been known that the optical hosts of luminous radio sources are primarily giant elliptical (gE and cD) galaxies (Matthews et al. 1964). In the more distant universe, indirect evidence that this association remains intact comes from the detection of normal elliptical host galaxies with $r^{1/4}$ law light profiles in *HST*/NICMOS observations of high-redshift radio galaxies (HzRGs) at $1 \lesssim z \lesssim 2$ (Pentericci et al. 2001; Zirm et al. 2003); the tendency for HzRGs to reside in moderately rich (proto-)cluster environments (Venemans et al. 2002; Stern et al. 2003); the spectacular (>100 kpc) luminous Lyα haloes seen around several sources, implying large gas reservoirs (Reuland et al. 2003; Villar-Martín et al. 2003); sub-mm detections of HzRGs, implying violent star formation activity up to $\sim 100\,\mathrm{M}_{\odot}\mathrm{yr}^{-1}$ (Archibald et al. 2001; Reuland et al. 2004); and a few direct kinematic measurements of HzRGs (Dey & Spinrad 1996). The most compelling evidence of this association of HzRGs with the most massive systems, however, is the tight correlation of the observed near-infrared Hubble, or $K-z$ diagram for powerful radio sources (De Breuck et al. 2002, Rocca-Volmerange et al. 2004): HzRGs form a narrow redshift sequence which traces the envelope of radio-quiet galaxies and is well-modeled by the evolution of a stellar population formed at high redshift from a reservoir of $10^{12}\,\mathrm{M}_{\odot}$. With the more recent discovery that the stellar bulge and central black hole masses of galaxies are closely correlated, it is no longer a surprise that the parent galaxies of the most powerful radio sources occupy the upper end of the galaxy mass function (Maggorian 1998; Tremaine 2002).

The peak of the stellar emission at 1.6 μm of elliptical galaxies has been found to be a reasonably robust measure of the stellar mass for old passively evolving systems. The mass-to-light ratio at this wavelength does not vary greatly for ages $\gtrsim$ 1Gyr. The *Spitzer Space Telescope* now allows us to observe this feature in distant sources in the rest frame. In particular the four bands of the IRAC instrument and the IRS 16 μm peak-up imager straddle the rest frame 1.6 μm flux density at $1 \leq z \leq 5$.

1.1. Sample Selection

In order to investigate the formation and evolution of the most massive galaxies we have performed a *Spitzer* survey of 70 HzRGs in GO cycle 1. These HzRGs have also been carefully chosen to cover the full range of redshifts from $z = 1$ to the redshift of the highest known radio galaxy ($z = 5.2$) and two orders of magnitude in radio luminosity, preferentially selecting targets with supporting data from *HST*, *Chandra* and SCUBA/MAMBO. By covering this parameter space, any trends with radio luminosity or redshift should be apparent. The observations consist of photometry in eight bands from the three instruments

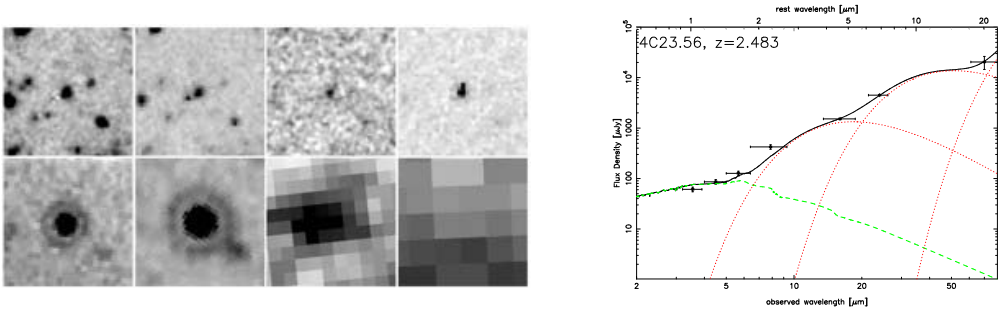

Figure 1. **(Left)** Postage stamp images of 4C23.56 at z=2.48: the 4 IRAC bands (top row - wavelength increasing left to right) followed by the IRS 16 μm peak-up image and the MIPS bands (bottom row) showing a clear detection in each waveband out to 70 μm **(Right)** SED fitting of 4C23.56 *Spitzer* data using an elliptical galaxy template and black-bodies of various temperatures.

aboard *Spitzer*, exercising the full complement of imaging capabilities (IRAC: 3.6, 4.5, 5.8 and 8 μm; IRS: 16 μm; MIPS: 24, 70 and 160μm). Due to uncertainty in the ability of MIPS to image against the Galactic infrared background at the time of submission of GO Cycle 1, we chose only to image 26/70 HzRGs with MIPS. The other 54 sources have been applied to be observed in *Spitzer* Cycle 3. The IRS images are only for the 46 objects above $z = 2$ as below this redshift the 8 μm IRAC channel adequately covers the longward side of the 1.6 μm bump.

The 'SHizRaG' team keep track of this project through a private webpage which we intend to make public eventually. Currently a restricted version of the webpage is available here:
`http://spider.ipac.caltech.edu/staff/seymour/SHizRaGs.html`

2. Stellar Luminosities and Masses

2.1. SED Fitting

In order to determine the 1.6 μm stellar luminosity, the contribution at this wavelength from hot, AGN heated dust needs to be ascertained. We have performed this analysis for the sample of 17 MIPS HzRGs which have 24 μm detections as well IRAC observations. For the modeling presented here we have chosen to use just the *Spitzer* data. The principle reason is that shorter wavelengths, *i.e.* the rest-frame optical, are more likely to have significant contributions from young stellar populations, emission lines, and AGN continuum.

We model the observed 3.6 to 24 μm data using an elliptical stellar template and three black-bodies. The elliptical stellar SED is taken from the PÉGASE (Fioc & Rocca-Volmerange 1997) software and corresponds to a passively evolving $10^{12}\,M_{\odot}$ stellar population formed at $z = 10$; *i.e.* for each redshift a template of the correct age was chosen although the SED does not evolve significantly after 1 Gyr (*i.e.* $z \sim 4.4$). The three black-bodies where chosen to be at 60 K (analogous to the temperature of cold dust found from sub-mm observations), 250 K and 600-1200 K. This last value was allowed to vary and the best temperature from the fitting applied. Full details of this modeling are presented in Seymour et al. (*in prep.*).

Figure 1 illustrates the *Spitzer* observations and the SED modeling for one representative source, 4C23.56 at $z = 2.48$. The best fit hot dust temperature is 750 K and one can see that the 1.6 μm stellar peak has considerable AGN contamination. A more detailed analysis of the broad-band, X-ray to radio SED of 4C23.56 is presented in De Breuck et al. (*in prep.*).

The other 53 HzRGs with no MIPS detections can at least provide upper limits to the stellar luminosities and, in some cases only the upper limits come from detections only in IRAC channels 1 and 2. So we fit a maximum elliptical template SED to the IRAC data. In some case the elliptical template fits quite well to IRAC channels 1-3 and in others the SED is steeply rising at the longer wavelengths and the fit is restricted only by channel 1. In the former case the we calculate a 'nominal' stellar mass from the fit, but in the later we may only derive upper limits.

2.2. Results

The derived rest-frame, AGN-subtracted, 1.6 μm stellar luminosities are shown against redshift in Fig. 3 (top) for all our HzRGs. Also laid on the plot by a solid line is the stellar luminosity of a $10^{12}\,M_{\odot}$ elliptical galaxy. The stellar luminosities imply stellar masses in the range $10^{11} - 10^{12}\,M_{\odot}$ with a mean mass of $\sim 10^{11.5}\,M_{\odot}$ (Fig. 3 bottom). This mean mass remains consistent out to $z = 3$ (beyond which the parameter space becomes less well sampled) suggesting that the upper end of the mass function is already in place by at least $z = 3$.

3. Mid-IR luminosities

Figure 3 shows the rest 6.75 μm luminosity against the rest 3 GHz luminosity for the 18 radio galaxies with MIPS observations. The wavelength of 6.75 μm was chosen as a fiducial mid-IR wavelength as it is the mean rest wavelength of the observed MIPS 24 μm band for our sample and also the wavelength of the LW2 filter from ISOCAM, allowing a direct comparison of derived luminosities. It is clear to first approximation that the two luminosities correlate and by implication have a common origin. This correlation makes sense if the radio luminosity comes from lobes induced by a jet from the AGN and the mid-IR comes from hot AGN-heated dust.

The mid-IR luminosities are also all greater than $10^{11} L_{\odot}$ implying bolometric luminosities on ULIRG scales assuming local relations hold for these objects. These radio galaxies tend to have a higher mean mid-IR to radio luminosity ratio then those selected at lower redshift, e.g., Ogle et al. (2006) finds that $z < 1$ radio galaxies tend to have $L_{\rm mid-IR}/L_{\rm radio} \sim 10 - 100$.

4. Conclusions and Future Work

We have presented a stellar-luminosity/redshift relation of HzRGs, a more physical representation of the $K - z$ diagram. This distribution seems to confirm the long held paradigm that radio galaxies are hosted by massive ellipticals out to high redshifts, and that the most massive galaxies are already in place by redshift 4 and possibly earlier. We also observe a correlation between the infrared and radio luminosities which is unsurprising if they are both fueled by the AGN.

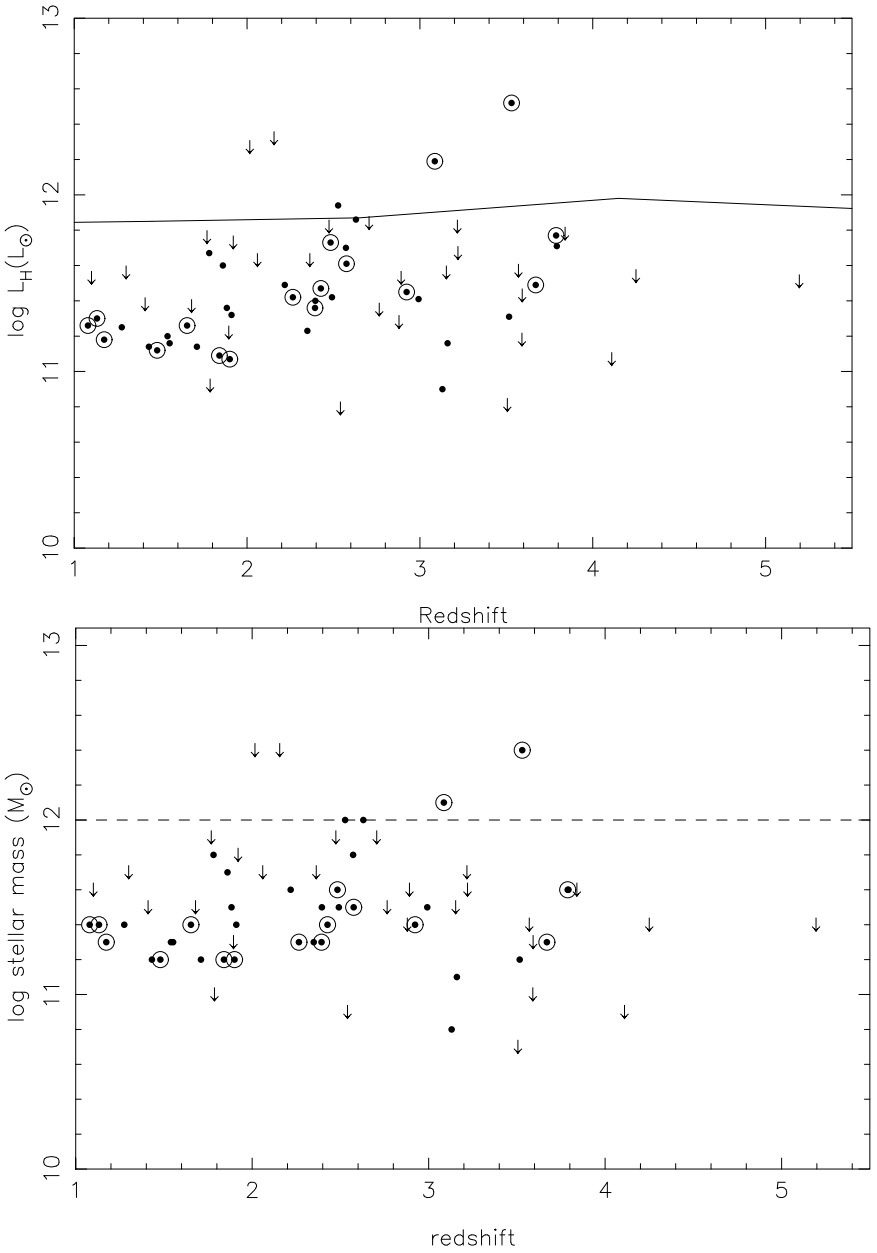

Figure 2. **(Top)** HzRG Stellar luminosities plotted against redshift of each HzRG. The solid line indicates a of $10^{12}\,M_\odot$ elliptical galaxy. **(Bottom)** Stellar masses from the SED fitting plotted against redshift. Most stellar luminosities indicate with stellar masses of $10^{11}-10^{12}\,M_\odot$. Stellar luminosities and masses derived from sources with MIPS 24 μm detections are circled, the dots with out circles are 'nominal' masses from just IRAC data. Downward arrows indicate upper limits.

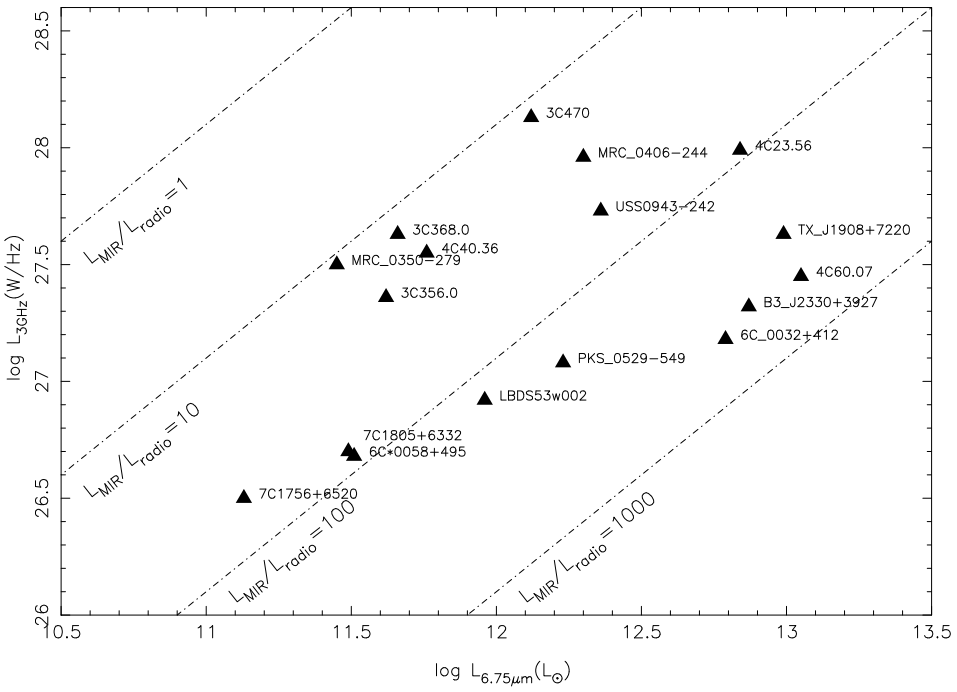

Figure 3. Rest mid-IR luminosity against rest radio luminosity which approximately correlate implying a common origin. This correlation may be explained by the AGN producing the radio jets and also heating the hot dust radiating in the mid-IR. The mid-IR/radio ratio increases at higher redshifts compared to low redshift samples (e.g., Ogle et al. 2006) most likely due to the hotter temperatures of the AGN-heated dust.

Current on-going work includes mm/sub-mm observations with SCUBA, MAMBO and the CSO to constrain the cold dust component at longer wavelengths and hence estimate the mass of this cold dust. Over-densities of sources around radio galaxies are being investigated to look for evidence of cluster formation (Zirm et al. *in prep.*). Over half the sources with $24\,\mu$m images have over-densities of factors of 2-5 greater than that expected from $24\,\mu$m source counts. These radio galaxies mainly lie at $1.5 < z < 2.5$ where the strong $6 - 8\,\mu$m PAH feature passes though the $24\,\mu$m MIPS band, enhancing the $24\,\mu$m flux density.

Acknowledgments. We thank the LOC for organising a great conference and were particularly impressed by the nifty design of the webpage. We also liked Harry's conference haircut.

References

Antonucci, R. 1993 *ARA&A*, **31**, 473A
Archibald, E. et al. 2001, *MNRAS*, **323**, 417
Blandford, R. & Payne, D. 1982, *MNRAS*, **199**, 883
De Breuck, C. et al. 2002, *AJ*, **123**, 637
De Breuck, C. et al. *in prep.*
Dey, A. & Spinrad, H. 1996, *AJ*, **459**, 133
Lacy, M. et al. 1994, *MNRAS*, **271**, 504
Matthews, T, et al. 1964, *ApJ*, **140**, 35
Pentericci, L. et al. 2001, *ApJS*, **135**, 63
Rees, M. 1978, *Nature*, **275**, 516
Reuland, M. et al. 2003, *ApJ*, **592**, 755
Reuland, M. et al. 2004, *MNRAS*, **353**, 377
Rocca-Volmerange, B. et al. *A&A*, **415**, 931
Seymour, N. et al. *AJ, in prep.*
Stern, D. et al. 2003, *AJ*, **125**, 2759
Venemans et al. 2002, *ApJ*, **596**, L11
Villar-Martín, M. et al. 2003, *MNRAS*, **346**, 273
Zirm, A., Dickinson, M. & Dey, A, 2003, *ApJ*, **585**, 90